XLVI CILAMCE
VITÓRIA - ES - BRAZIL - 2025
XLVI IBERO-LATIN AMERICAN CONGRESS ON COMPUTATIONAL METHODS IN ENGENEERING

Theoretical study of human-structure interaction during crowd jumping

Phablo V. I. Dias[1,2], Zenón J. G. N. del Prado[1]

[1]*School of Civil and Environmental Engineering, Federal University of Goiás*
Avenida Universitária, 1488, Setor Leste Universitário, 74605-200, Goiânia, Goiás, Brazil
phablo@discente.ufg.br, zenon@ufg.br

[2]*Dept. of Civil Engineering, Federal Institute of Education, Science and Technology of Goiás*
Rua 75, 46, Setor Central, 74055-110, Goiânia, Goiás, Brazil
phablo.dias@ifg.edu.br

Abstract. This study presents a time-domain model for crowd-structure interaction in which each jumper is represented as an individual spring-mass-damper system coupled to a rectangular plate. The formulation accounts for contact loss during jumping and enables independent control of the dynamic force generated by each participant. Numerical simulations on a simply supported plate investigated two factors affecting the dynamic response: passive interaction and frequency detuning. Results showed that increasing the number of passive jumpers reduces plate accelerations due to lower energy input, while detuning decreases the overall response but can introduce additional resonance peaks related to structural harmonics. The findings demonstrate that both the proportion of passive or detuned individuals and the detuning magnitude are key parameters influencing vibration serviceability, and that the proposed model effectively captures individual-level interaction effects.

Keywords: Human-structure interaction, Crowd jumping, Human-induced loading

1 Introduction

The increasing use of high-strength and lightweight materials has enabled the construction of floors with larger spans, reduced mass, and fewer non-structural partitions, resulting in more flexible structures with progressively lower natural frequencies and damping ratios [1, 2]. In this context, dynamic human activities have become a relevant concern for the vibration serviceability of such structures. Among these activities, synchronized crowd jumping produces the highest demands, especially when coordinated by auditory or visual stimuli, as observed in concerts and sporting events [3]. Inadequate consideration of these excitations can compromise structural performance and safety, lead to significant economic losses, and in extreme situations pose risks to occupant integrity.

During rhythmic group activities, the applied forces act predominantly in the vertical direction and exhibit variations both among individuals and over time. Inter-subject variability arises from differences in movement patterns among people, while intra-subject variability is associated with changes in load parameters for the same individual over the course of the activity [4]. These variations generate an energy spread around the load harmonics [5], which can distort the predicted structural response by overestimating resonant effects and underestimating non-resonant conditions when simplified models are used [6]. Incorporating these effects into load models is essential for accurate predictions of the dynamic response.

In addition to producing external excitations, the presence of a crowd alters the dynamic properties of the structure, a phenomenon referred to as human-to-structure interaction (H2SI). Studies have shown that human occupancy can modify natural frequencies and increase structural damping [7, 8]. Conversely, structural vibrations can influence the movement patterns of occupants, thereby changing the applied loads, a process known as structure-to-human interaction (S2HI). These reciprocal effects are jointly referred to as human-structure interaction (HSI), which is a key aspect in the analysis of floors subjected to collective rhythmic excitations.

Experimental studies highlight synchronization as a critical factor. An et al. [9] observed that the most severe condition for a composite floor occurred when a crowd jumped in synchrony, resulting in the highest acceleration levels among the activities investigated. Similarly, Lee et al. [10] reported an event in Seoul where rhythmic movements in a fitness center on the 12th floor of a 39-story building induced vertical vibrations lasting ten minutes,

leading to panic and evacuation of the occupants.

Modeling HSI typically involves formulating the equations of motion for the coupled crowd-structure system. A mechanical representation of the human body is adopted for this purpose. The spring-mass-damper (SMD) model is widely used due to its simplicity and ability to capture the influence of the human body on the structural dynamic properties [11]. More advanced configurations have been proposed in which the crowd is represented by multiple individual SMDs coupled to a multi-degree-of-freedom (MDOF) structural model [12, 13]. However, these approaches do not explicitly account for individual loss of contact between jumpers and the floor, nor do they allow the independent control of the force generated by each jumper's musculoskeletal system during jumping.

The present study proposes a time-domain mathematical model for crowd-structure interaction, where each jumper is individually represented by an SMD model coupled to a rectangular plate. The formulation enables the computation of responses for both the plate and the jumpers. An external load is applied directly to each SMD to represent the compression and extension phases during jumping. The coupled system is solved as a piecewise smooth contact problem, allowing the individual verification of contact loss for each jumper throughout the activity.

2 Mathematical formulation

The crowd is represented by N_s spring–mass–damper (SMD) oscillators, where each k-th oscillator represents one jumper with a single generalized coordinate $w_h^{(k)}$, modal mass $m_h^{(k)}$, stiffness $k_h^{(k)}$, and damping $c_h^{(k)}$, positioned at point (x_k, y_k) on the structural floor. The floor is modeled as a simply supported rectangular plate under the Kirchhoff–Love assumptions, with in-plane dimensions a and b, thickness h, density ρ, Young's modulus E, and displacement fields $u(x, y, t)$, $v(x, y, t)$, and $w(x, y, t)$ in the x-, y-, and z-directions, respectively. A schematic of the plate and the SMD arrangement is shown in Fig. 1.

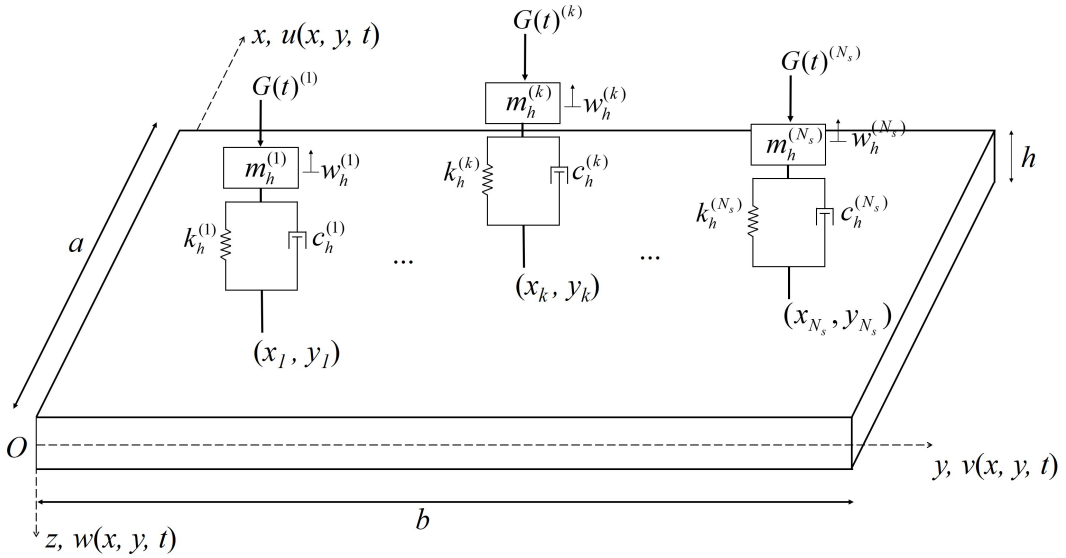


Figure 1. Rectangular plate with the crowd model.

Based on study of the Dias and Del Prado [14], the formulation follows Lagrange's equations, and the total potential energy U and kinetic energy T of the coupled system can be written as

$$\begin{aligned} U \;=\; & \frac{E\,h}{2\,(1-\nu^2)} \int_0^a \int_0^b \left(\varepsilon_{x,0}^2 + \varepsilon_{y,0}^2 + 2\,\nu\,\varepsilon_{x,0}\,\varepsilon_{y,0} + \frac{1-\nu}{2}\,\gamma_{xy,0}^2 \right) dy\,dx \\ & + \frac{E\,h^3}{24\,(1-\nu^2)} \int_0^a \int_0^b \left(\kappa_x^2 + \kappa_y^2 + 2\,\nu\,\kappa_x\,\kappa_y + \frac{1-\nu}{2}\,\kappa_{xy}^2 \right) dy\,dx \\ & + \frac{1}{2} \sum_{k=1}^{N_s} k_h^{(k)} \left(w_h^{(k)} - w(x_k, y_k, t) \right)^2, \end{aligned} \tag{1}$$

$$T \;=\; \frac{1}{2}\,\rho\,h \int_0^a \int_0^b \left(\dot{u}^2(x,y,t) + \dot{v}^2(x,y,t) + \dot{w}^2(x,y,t) \right) dy\,dx \;+\; \frac{1}{2} \sum_{k=1}^{N_s} m_h^{(k)} \left(\dot{w}_h^{(k)} \right)^2. \tag{2}$$

The plate is modeled with viscous damping by the Rayleigh dissipation function [15]. The SMD oscillators follow the same approach [16]. The total dissipation is

$$\begin{aligned}\mathcal{R} \;&= \zeta_p\,\omega_{i,j}\,m_j \int_0^a\!\!\int_0^b \left(\dot{u}^2(x,y,t) + \dot{v}^2(x,y,t) + \dot{w}^2(x,y,t)\right)\,dy\,dx,\\ &+ \sum_{k=1}^{N_s} \zeta_h^{(k)}\,\omega_h^{(k)}\,m_h^{(k)}\left(\dot{w}_h^{(k)} - \dot{w}(x_k,y_k,t)\right)^2.\end{aligned} \tag{3}$$

where, ζ_p is the viscous damping ratio of the plate at the i,j-th mode with natural frequency $\omega_{i,j}$ and modal mass m_j; analogously, $\zeta_h^{(k)}$, $\omega_h^{(k)}$, and $m_h^{(k)}$ are the damping ratio, natural frequency, and modal mass of jumper k.

As studied in [14], a harmonic force is applied to each SMD generalized coordinate to represent the compression and propulsion generated by the jumper during rhythmic movements. The static weight $m_h\,g$ is also included. The work W of the external forces ($G(t)$) acting on the SMDs is

$$W \;= \sum_{k=1}^{N_s} {w_h}^{(k)}\left(\Gamma^{(k)}\,m_h^{(k)}\,g\sin(\Omega^{(k)}t) \;-\; m_h^{(k)}\,g\right), \tag{4}$$

where $\Gamma^{(k)}$ and $\Omega^{(k)}$ are the amplitude and excitation frequency of the propulsion force for k-th jumper, g is the gravitational acceleration, and ${w_h}^{(k)}$ and ${m_h}^{(k)}$ are the generalized displacement and modal mass of k-th jumper.

The plate is assumed to be simply supported in the vertical direction and has fixed edges in the axial direction, leading to the selection of the following displacement fields $u(x,y,t)$, $v(x,y,t)$, and $w(x,y,t)$ in the axial and transverse directions, which satisfy the boundary conditions [15]:

$$u(x,y,t) = \sum\nolimits_{m=1}^{M_u}\sum\nolimits_{n=1}^{N_u} u_{m,n}(t)\,\sin\left(\frac{2\,m\,\pi\,x}{a}\right)\sin\left(\frac{2\,n\,\pi\,y}{b}\right); \tag{5}$$

$$v(x,y,t) = \sum\nolimits_{m=1}^{M_v}\sum\nolimits_{n=1}^{N_v} v_{m,n}(t)\,\sin\left(\frac{2\,m\,\pi\,x}{a}\right)\sin\left(\frac{2\,n\,\pi\,y}{b}\right); \tag{6}$$

$$w(x,y,t) = \sum\nolimits_{m=1}^{M_w}\sum\nolimits_{n=1}^{N_w} w_{m,n}(t)\,\sin\left(\frac{m\,\pi\,x}{a}\right)\sin\left(\frac{n\,\pi\,y}{b}\right), \tag{7}$$

where m and n are the half-wave numbers in the x and y directions, respectively; M_u, N_u, M_v, N_v, M_w, and N_w are the number of terms used in each displacement field; $u_{m,n}(t)$, $v_{m,n}(t)$, and $w_{m,n}(t)$ are the unknown amplitudes.

The generalized displacement vector of the empty plate is

$$\mathbf{q} = \left[u_{1,1}(t),\ldots,u_{M_u,N_u}(t),\; v_{1,1}(t),\ldots,v_{M_v,N_v}(t),\; w_{1,1}(t),\ldots,w_{M_w,N_w}(t)\right]^T, \tag{8}$$

whose size is $N_q = N_u + N_v + N_w$, where N_u, N_v, and N_w are the numbers of modal coordinates associated with the u-, v-, and w-fields, respectively. A generic component is denoted q_j with $1 \le j \le N_q$. Each jumper contributes one extra degree of freedom, so the system size becomes $\tilde{N} = N_q + N_s$. The coordinate associated with the k-th jumper is denoted $q_{\tilde{N}}^{(k)}$.

In order to derive the set of nonlinear dynamic equations, the Rayleigh-Ritz method is employed in conjunction with the Hamiltonian principle [14, 17]. Then, the nonlinear equations of motion can be written as:

$$\begin{aligned}&m_j\,\ddot{q}_j + \sum_{i=1}^{N_q} c_{i,j}\,\dot{q}_i + \sum_{i=1}^{N_q} k_{i,j}\,q_i + \sum_{i,k=1}^{N_q} k_{jik}\,q_i\,q_k + \sum_{i,k,l=1}^{N_q} k_{jikl}\,q_i\,q_k\,q_l\\ &= \sum_{k=1}^{N_s}\left[k_h^{(k)}\left(q_{\tilde{N}}{}^{(k)} - \sum_{i=1}^{N_q} q_i\,\psi_i^{(k)}\right)\psi_j^{(k)} \;+\; c_h^{(k)}\left(\dot{q}_{\tilde{N}}^{(k)} - \sum_{i=1}^{N_q}\dot{q}_i\,\psi_i^{(k)}\right)\psi_j^{(k)}\right],\end{aligned} \tag{9}$$

$$m_h^{(k)}\,\ddot{q}_{\tilde{N}}^{(k)} + c_h^{(k)}\left(\dot{q}_{\tilde{N}}^{(k)} - \sum\nolimits_{i=1}^{N_q}\dot{q}_i\,\psi_i^{(k)}\right) + k_h^{(k)}\left(q_{\tilde{N}}^{(k)} - \sum\nolimits_{i=1}^{N_q} q_i\,\psi_i^{(k)}\right) = (\Gamma^{(k)}\sin(\Omega^{(k)}\,t) - 1)\,m_h^{(k)}\,g; \tag{10}$$

where the modal mass of the plate is given by $m_j = \frac{1}{4},\rho,a,b,h$; the modal damping coefficient of the plate is $c_{i,j} = 2\,\zeta_p\,\omega_{i,j}\,m_j$; $k_{i,j}$, $k_{j,i,k}$, and $k_{j,i,k,l}$ are stiffness terms representing linear, quadratic, and cubic nonlinearities of the plate, respectively; $\psi_i^{(k)} = \psi_i(x_k,y_k)$ denotes the i-th plate mode shape evaluated at the position of k-th jumper; the modal damping coefficient of the jumper is $c_h^{(k)} = 2\,\zeta_h^{(k)}\,\omega_h^{(k)}\,m_h^{(k)}$.

For numerical implementation, the coupled system is divided by the mass terms and rewritten in state-space form. Defining $\mathbf{y}_p = \dot{\mathbf{q}}$ and $y_h^{(k)} = \dot{q}_{\tilde{N}}^{(k)}$ as the vertical velocities of the plate and the k-th jumper, respectively, the contact-phase equations become

$$\begin{cases} \dot{\mathbf{q}} = \mathbf{y}_p; \\ \dot{\mathbf{y}}_p = -\mathbf{M}^{-1}\big(\mathbf{C}\dot{\mathbf{q}} + \big(\mathbf{K1} + \mathbf{K2}(q) + \mathbf{K3}(q,q)\big)\mathbf{q}\big) + \sum_{k=1}^{N_s} A_{\mathrm{HSI}}^{(k)}; \\ \dot{q}_{\tilde{N}}^{(k)} = y_h^{(k)}; \\ \dot{y}_h^{(k)} = \mathrm{GRF}^{(k)}/m_h^{(k)} + (\Gamma^{(k)}\,\sin(\Omega^{(k)}\,t) - 1)g. \end{cases} \tag{11}$$

where $\mathbf{M}$ and $\mathbf{C}$ are the mass and damping matrices, and $\mathbf{K}_1$, $\mathbf{K}_2(\mathbf{q})$, and $\mathbf{K}_3(\mathbf{q},\mathbf{q})$ are the linear, quadratic, and cubic stiffness matrices of the empty plate.

$A_{\mathrm{HSI}}^{(k)}$ is the acceleration transmitted from the k-th jumper to the plate, written as

$$A_{HSI}^{(k)} = \lambda^{(k)} \left(2\,\zeta_h^{(k)}\,\omega_h^{(k)} \left(\dot{q}_{\tilde{N}}^{(k)} - \sum_{i=1}^{N_q} \dot{q}_i\,\psi_i^{(k)} \right) + (\omega_h^2)^{(k)} \left(q_{\tilde{N}}^{(k)} - \sum_{i=1}^{N_q} q_i\,\psi_i^{(k)} \right) \right), \tag{12}$$

where $\lambda^{(k)} = m_h^{(k)}/m_j$ is the mass ratio between the k-th jumper and the structure.

According Dias and Del Prado [17], during contact the jumper exerts a ground reaction force (GRF) on the plate and it is expected that this force is zero in the flight phase. GRF is generated while the jumper alternates between leg flexion and extension in preparation for take-off. Evaluating Eq. (10) with the jumper's inertial and external forcing terms set to zero gives

$$\mathrm{GRF}^{(k)} = c_h^{(k)} \left(\sum_{i=1}^{N_q} \dot{q}_i\,\psi_i^{(k)} - \dot{q}_{\tilde{N}}^{(k)} \right) + k_h^{(k)} \left(\sum_{i=1}^{N_q} q_i\,\psi_i^{(k)} - q_{\tilde{N}}^{(k)} \right). \tag{13}$$

The system is formulated as piecewise smooth, alternating between contact and flight phases [17, 18]. Numerical integrations employs a fourth-order Runge–Kutta method with event detection for every jumper: take-off occurs when $\mathrm{GRF}^{(k)} \leq 0$ and touch-down when $\mathrm{GRF}^{(k)} > 0$. During the flight of the k-th jumper, each corresponding interaction term is set to $A_{HSI}^{(k)} = 0$, and only gravity is considered. The corresponding state-space representation for all jumper in flight-phase is

$$\begin{cases} \dot{\mathbf{q}} = \mathbf{y}_p; \\ \dot{\mathbf{y}}_p = -\mathbf{M}^{-1}\Big(\mathbf{C}\,\dot{\mathbf{q}} + \big(\mathbf{K}_1 + \mathbf{K}_2(\mathbf{q}) + \mathbf{K}_3(\mathbf{q},\mathbf{q})\big)\mathbf{q}\Big); \\ \dot{q}_{\tilde{N}}^{(k)} = y_h^{(k)}; \\ \dot{y}_h^{(k)} = -\,g. \end{cases} \tag{14}$$

3 Numerical results

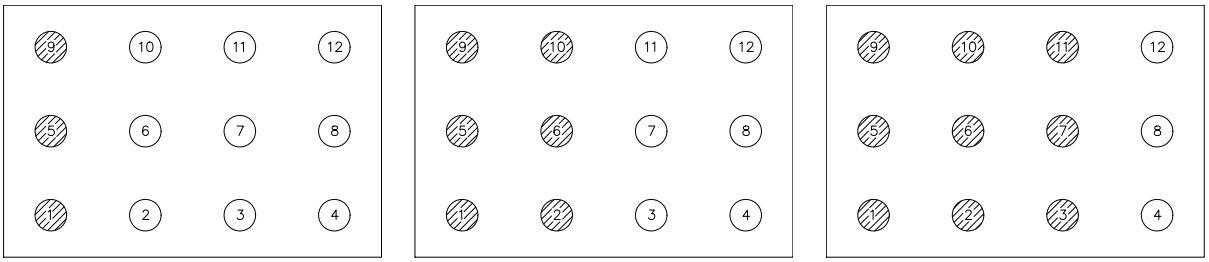
The numerical investigations consider a simply supported plate with in-plane displacements restrained. The plate dimensions are $a = 12.0\,\mathrm{m}$, $b = 8.0\,\mathrm{m}$, and thickness $h = 0.20\,\mathrm{m}$. The material is isotropic with properties $E = 21\,\mathrm{GPa}$, $\rho = 2500\,\mathrm{kg/m^3}$, and $\nu = 0.20$. Structural damping is modeled as viscous, with the same modal coefficient for all modes [19], $\xi_p = 0.025$. These parameters yield a fundamental frequency of $\omega_{1,1} = 6.0\,\mathrm{Hz}$, which is below the serviceability ranges specified by several design codes for floors subjected to harmonic excitation from jumpers. The adopted values are consistent with floors commonly reported in experimental crowd studies, such as those by Sousa et al. [20] and Xiong et al. [21].

The plate was discretized using $N_q = 16$ generalized coordinates, following the same formulation as in [14]. Each jumper was assigned the same modal mass, $m_h = 75\,\mathrm{kg}$, and a leg stiffness $k_h(\Omega_s)$ computed from the nonlinear frequency-dependent function given in equation (15) according [22]. A propulsion force amplitude $\Gamma = 1.5$ and a modal damping ratio $\zeta_h = 0.30$ were adopted for all oscillators.

$$k_h = 61.2 - 94.3\,\Omega_s + 53.1\,\Omega_s^2 - 8.36\,\Omega_s^3. \tag{15}$$

Two factors with potential to significantly influence the plate response were investigated: passive interaction, in which part of the crowd does not apply dynamic force to the floor, and frequency detuning, where some jumpers perform the motion at a cadence slightly different from the target frequency. The initial analysis considered only

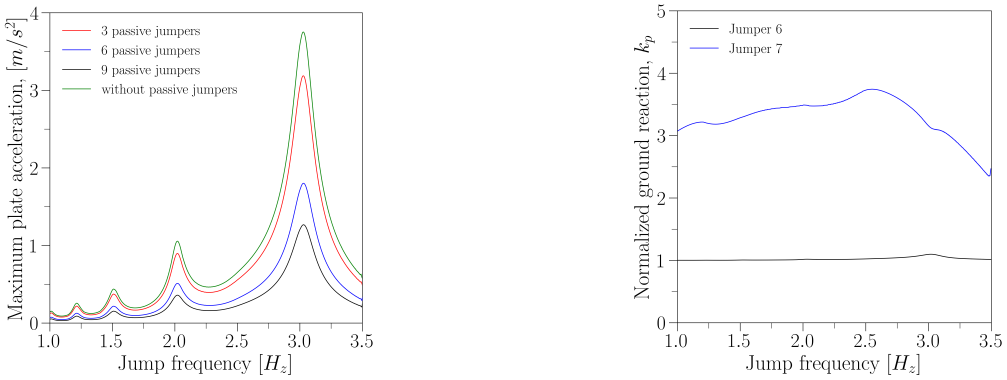
passive interaction, with all active individuals tuned to the same frequency. To reduce computational cost while maintaining representativeness, a configuration with twelve jumpers was adopted, as shown in Figure 2. Shaded jumpers represent passive participants, for whom $\Gamma = 0$. Three configurations were analyzed with 3, 6, and 9 passive jumpers. The jumpers were spaced 3.00 m apart and positioned 1.50 m from the plate edges in the horizontal direction. In the vertical direction, they were placed 1.33 m from the edges and 2.67 m apart.



(a) Three passive jumpers (b) Six passive jumpers (c) Nine passive jumpers

Figure 2. Arrangement of 12 jumpers with passive interaction.

Figure 3 shows the plate acceleration for each passive interaction configuration along with the reference case where all jumpers are active. A prominent peak appears at 3.0 Hz, which corresponds to the 1/2 subharmonic of the plate's fundamental frequency $\omega_{1,1} = 6.0$ Hz. Other subharmonics of orders 1/3, 1/4, and 1/5 are visible at 2.0, 1.5, and 1.2 Hz, respectively. As the number of passive jumpers increases, the maximum plate acceleration decreases because the number of active exciters is reduced and consequently the energy input to the system diminishes. To assess the local effect, the ground reaction force normalized by the jumper weight ($kp = \mathrm{GRF}/g\,m_h$) of jumpers 6 and 7 were monitored for the case with 6 passive jumpers. Figure 3b shows that jumper 7, who is active, produces a dynamic load consistent with values reported in the literature [22, 23], while jumper 6, who is passive, applies only the static load due to body weight, corresponding to $kp = 1$.



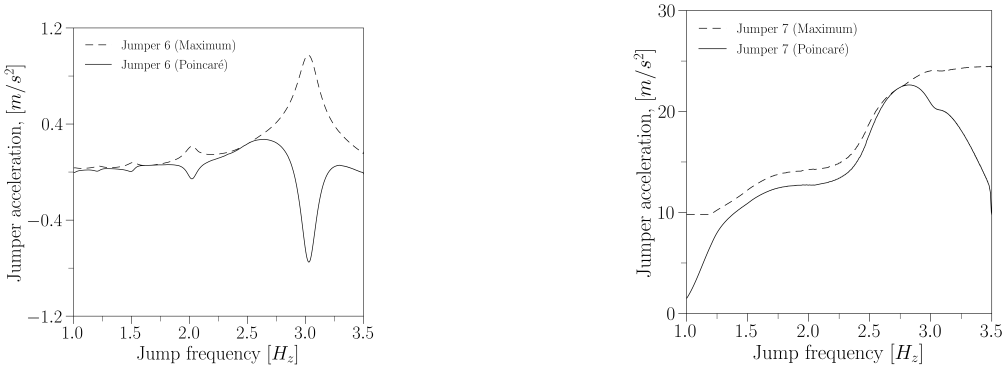
(a) (b)

Figure 3. Influence of passive jumpers on the system response: (a) plate acceleration for increasing number of passive jumpers and (b) normalized ground reaction for passive and active jumpers.

Analysis of the jumper accelerations in Figure 4 shows that jumper 6 reproduces the plate motion with lower amplitude since there is no loss of contact and therefore no inertial reinforcement during landing. As a result, negative values appear in the Poincaré section, associated with the oscillatory motion imposed by the structure. The response of jumper 7, on the other hand, exhibits a hill-shaped pattern [23], as expected.

Figure 5 presents the plate acceleration response when frequency detuning is considered. In this case, all jumpers have $\Gamma = 1.5$ but the same shaded jumpers from Figure 2 now jump at frequencies 5%, 15%, and 25% below the target frequency. The results show that the highest plate response occurs in the fully synchronized case. As detuning increases, the overall response decreases and additional resonance peaks may appear, indicating interactions with other structural harmonics.

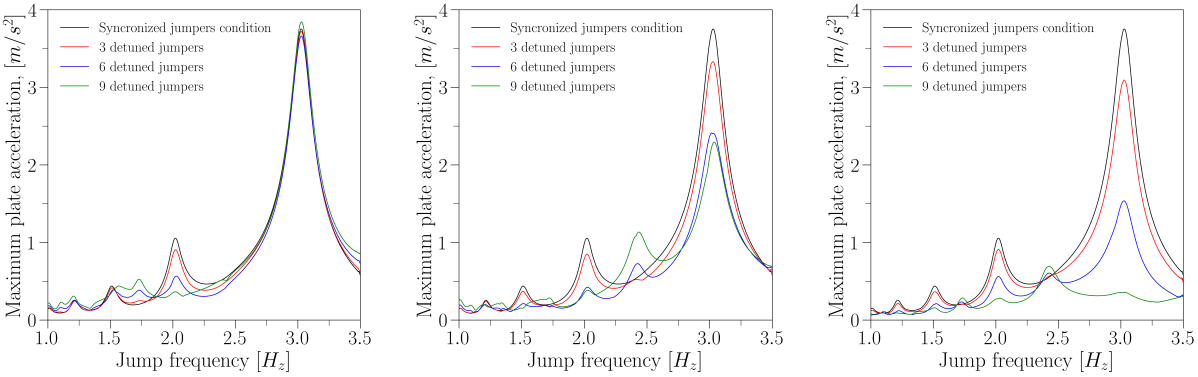
Figure 6 shows the normalized ground reaction force for jumper 7 under each detuning condition. The responses are similar for the lowest detuning ratios but diverge significantly at the highest variation with 25% detuning and nine detuned jumpers. This indicates that both the number of detuned individuals and the magnitude of detuning are relevant to the dynamic interaction and resulting structural response.



(a) Jumper 6 in passive interaction

(b) Jumper 7 in active interaction

Figure 4. Accelerations of jumpers in the passive interaction configuration with 6 passive idividuals: (a) jumper 6 and (b) jumper 7.

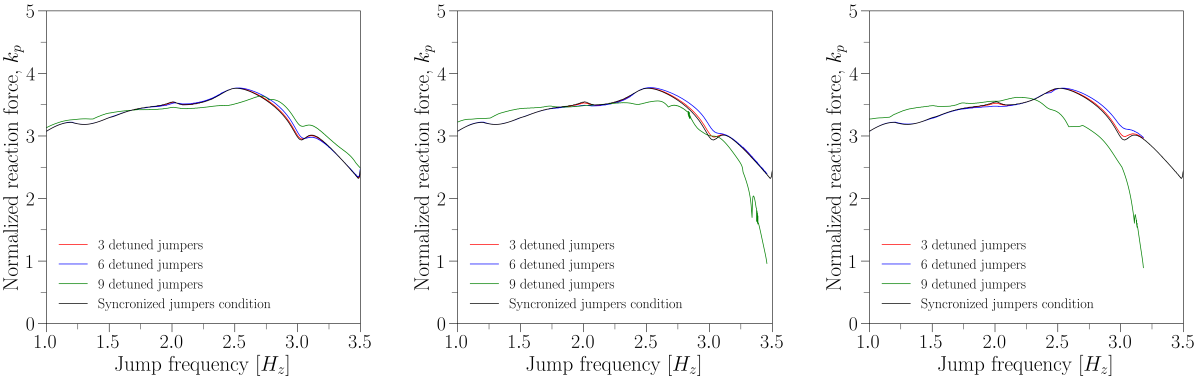


(a) Detuning ratio = 5%

(b) Detuning ratio = 15%

(c) Detuning ratio = 25%

Figure 5. Plate acceleration response for jumpers detuned below the target frequency.



(a) Detuning ratio = 5%

(b) Detuning ratio = 15%

(c) Detuning ratio = 25%

Figure 6. Normalized ground reaction force k_p for jumper 7 under detuning conditions below the target frequency.

4 Conclusions Remarks

A time-domain model for crowd-structure interaction was presented in this paper, representing each jumper as an individual spring-mass-damper system coupled to a rectangular plate and allowing explicit control of contact loss and dynamic force generation. Numerical analyses on a simply supported plate examined passive interaction and frequency detuning. Increasing the number of passive jumpers reduced plate accelerations due to lower energy input, while detuning decreased overall response but could introduce additional resonance peaks linked to other structural harmonics. The results highlight that both the proportion of passive or detuned individuals and the detuning magnitude significantly influence the dynamic behavior, and that the proposed formulation captures individual-level effects, offering a basis for broader applications in vibration serviceability studies.

Acknowledgements. The authors acknowledge the financial support of the Brazilian research agencies CAPES and CNPq. vspace12pt

Authorship statement. The authors hereby confirm that they are the sole liable persons responsible for the authorship of this work, and that all material that has been herein included as part of the present paper is either the property (and authorship) of the authors, or has the permission of the owners to be included here.

References

[1] S. Živanović, A. Pavic, and P. Reynolds. Vibration serviceability of footbridges under human-induced excitation: a literature review. *Journal of sound and vibration*, vol. 279, n. 1-2, pp. 1–74, 2005.

[2] C. Jones, P. Reynolds, and A. Pavic. Vibration serviceability of stadia structures subjected to dynamic crowd loads: A literature review. *Journal of Sound and Vibration*, vol. 330, n. 8, pp. 1531–1566, 2011.

[3] V. Racic and A. Pavic. Stochastic approach to modelling of near-periodic jumping loads. *Mechanical systems and signal processing*, vol. 24, n. 8, pp. 3037–3059, 2010a.

[4] Y. El Asri, M. Couchaux, M. Hjiaj, and M. Lukić. Spectral modelling approach for crowd-rhythmic activities performed on steel-concrete composite floors. *Engineering Structures*, vol. 299, pp. 117066, 2024.

[5] V. Racic and A. Pavic. Mathematical model to generate near-periodic human jumping force signals. *Mechanical Systems and Signal Processing*, vol. 24, n. 1, pp. 138–152, 2010b.

[6] J. Xiong and J. Chen. Power spectral density function for individual jumping load. *International Journal of Structural Stability and Dynamics*, vol. 18, n. 02, pp. 1850023, 2018.

[7] R. Sachse, A. Pavic, and P. Reynolds. Parametric study of modal properties of damped two-degree-of-freedom crowd–structure dynamic systems. *Journal of Sound and Vibration*, vol. 274, n. 3, pp. 461–480, 2004.

[8] E. Shahabpoor, A. Pavic, and V. Racic. Interaction between walking humans and structures in vertical direction: A literature review. *Shock and vibration*, vol. 2016, 2016.

[9] Q. An, Q. Ren, H. Liu, X. Yan, and Z. Chen. Dynamic performance characteristics of an innovative cable supported beam structure–concrete slab composite floor system under human-induced loads. *Engineering Structures*, vol. 117, pp. 40–57, 2016.

[10] K. Lee, S. H. Lee, G. C. Kim, and S. S. Woo. Global vertical resonance phenomenon between steel building and human rhythmic excitations. *Journal of Constructional Steel Research*, vol. 92, pp. 164–174, 2014.

[11] C. C. Caprani and E. Ahmadi. Formulation of human–structure interaction system models for vertical vibration. *Journal of Sound and Vibration*, vol. 377, pp. 346–367, 2016.

[12] C. Gallegos-Calderón, J. Naranjo-Pérez, C. M. C. Renedo, and I. M. Díaz. A frequency-domain approach to model vertical crowd-structure interaction in lightweight footbridges. *Journal of Sound and Vibration*, vol. 557, pp. 117750, 2023.

[13] E. Shahabpoor and A. Pavic. Human-structure dynamic interactions: Identification of two-degrees-of-freedom walking human model. *Journal of Sound and Vibration*, vol. 569, pp. 117974, 2024.

[14] P. V. I. Dias and Z. J. G. N. Del Prado. Theoretical analysis of human rhythmic jumping on oscillating floors. In *XLV Ibero-Latin American Congress on Computational Methods in Engineering, Maceió, AL, Brazil*, 2024.

[15] M. Amabili. *Nonlinear vibrations and stability of shells and plates*. Cambridge University Press, 2008.

[16] P. V. I. Dias and Z. J. G. N. Del Prado. Human-structure interaction during jumping on rectangular plates. In *XLIII Ibero-Latin American Congress on Computational Methods in Engineering, Foz do Iguaçu, PR, Brazil*, 2022.

[17] P. V. Dias and Z. J. Del Prado. Human–structure interaction during rhythmic jumping on rectangular plates subjected to time-dependent base excitation. *International Journal of Solids and Structures*, vol. 321, pp. 113504, 2025.

[18] R. E. White, N. A. Alexander, J. H. Macdonald, and A. R. Champneys. Parametric exploration of a simple model of human jumping on an oscillating structure. *Journal of Sound and Vibration*, vol. 509, pp. 116227, 2021a.

[19] M. Amabili. Nonlinear damping in nonlinear vibrations of rectangular plates: Derivation from viscoelasticity and experimental validation. *Journal of the Mechanics and Physics of Solids*, vol. 118, pp. 275–292, 2018.

[20] F. A. d. Sousa, G. L. Debona, and J. G. S. d. Silva. Dynamic analysis of floors subjected to rhythmic human activities based on the use of biodynamic models: numerical and experimental modelling. *IBRACON Journal of Structures and Materials*, vol. 17, n. 4, pp. e17402, 2023.

[21] J. Xiong, J. Chen, and C. Caprani. Spectral analysis of human-structure interaction during crowd jumping. *Applied Mathematical Modelling*, vol. 89, pp. 610–626, 2021.

[22] R. E. White, J. H. Macdonald, and N. A. Alexander. A nonlinear frequency-dependent spring-mass model for estimating loading caused by rhythmic human jumping. *Engineering Structures*, vol. 241, pp. 112229, 2021b.

[23] M. G. McDonald and S. Živanović. Measuring ground reaction force and quantifying variability in jumping and bobbing actions. *Journal of Structural Engineering*, vol. 143, n. 2, pp. 04016161, 2017.